Quantum Frontiers

上海交通大学
SHANGHAI JIAO TONG UNIVERSITY

李政道研究所
Tsung-Dao Lee Institute

ORIGINAL ARTICLE   **Open Access**

Check for updates

Is spontaneous vortex generation in superconducting 4Hb-TaS$_2$ from vison-vortex nucleation with $\mathbb{Z}_2$ topological order?

Rui Leonard Luo[2] and Gang V. Chen[1,3]* (ID)

Abstract

We propose the superconducting van der Waals material 4Hb-TaS$_2$ to realize the $\mathbb{Z}_2$ topological order and interpret the recent discovery of the spontaneous vortex generation in 4Hb-TaS$_2$ as the vison-vortex nucleation. For the alternating stacking of metallic/superconducting and Mott insulating layers in 4Hb-TaS$_2$, we expect the local moments in the Mott insulating 1T-TaS$_2$ layer to form the $\mathbb{Z}_2$ topological order. The spontaneous vortex generation in 4Hb-TaS$_2$ is interpreted from the transition or nucleation between the superconducting vortex and the $\mathbb{Z}_2$ vison in different phase regimes. Differing from the single vison-vortex nucleation in the original Senthil–Fisher's cuprate proposal, we consider such nucleation process between the superconducting vortex lattice and the vison crystal. We further propose experiments to distinguish this proposal with the $\mathbb{Z}_2$ topological order from the chiral spin liquid scenarios.

Keywords: $\mathbb{Z}_2$ topological order, Vison, Magnetic vortex, Magnetic memory effect
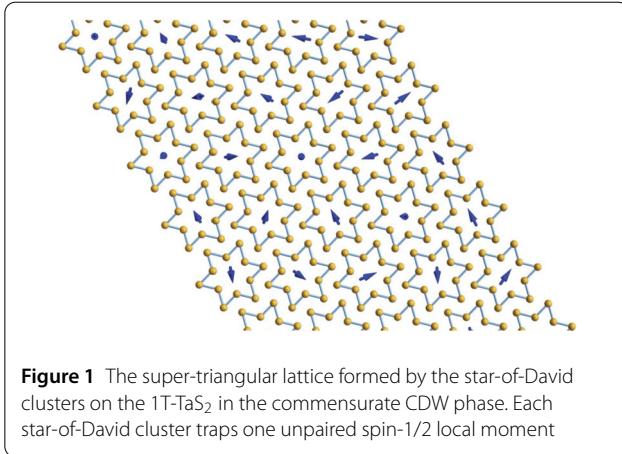
1 Introduction

Detecting the intrinsic topological orders and the emergent electron fractionalization is an interesting and challenging task. There have been a tremendous effort to identify topological orders and the associated electron fractionalization [1]. Among these efforts, symmetry has been quite useful in both classifying distinct topological orders and the identifications of measurable physical quantities [2–5]. One important consequence of the symmetries in topological orders is the quantum number fractionalization, and one such application is the charge fractionalization in the fractional quantum Hall liquid [6, 7]. The crystallographic symmetry has also proved to be quite useful in identifying the crucial features in the spectrum of the anyonic quasiparticles [2, 4], and this is related to

the crystal symmetry fractionalization in the topologically ordered phases. Another interesting effort is to trace the genesis of various exotic quasiparticles in the proximate phases [8–12]. This is of the fundamental importance to clarify the relationship between the topological phases and the proximate conventional states and to understand the nature of the phase transitions [12–14]. More specifically, in the context of the cuprates where the topological order was suggested and remains elusive, Senthil and Fisher proposed a creative scheme to trace the nucleation between the vison in $\mathbb{Z}_2$ topological order and the superconducting vortex [9]. Although this vortex-memory effect was found to be absent in cuprates [15], this idea remains to be an ingenious attempt to detect the topological order beyond fractional quantum Hall liquids. In this work, we propose the superconducting van der Waals material 4Hb-TaS$_2$ [16, 17] to be a physical platform for the $\mathbb{Z}_2$ topological order, and interpret the recently-discovered magnetic memory effect and the spontaneous vortex generation [16] as the vison-vortex nucleation due to the $\mathbb{Z}_2$ topological order. Our proposal for 4Hb-TaS$_2$ is a vortex lattice version

*Correspondence: chenxray@pku.edu.cn
[1] International Center for Quantum Materials, School of Physics, Peking University, Beijing, 100871, China
[3] Collaborative Innovation Center of Quantum Matter, Beijing, 100871, China
Full list of author information is available at the end of the article

Springer

Figure 1 The super-triangular lattice formed by the star-of-David clusters on the 1T-TaS$_2$ in the commensurate CDW phase. Each star-of-David cluster traps one unpaired spin-1/2 local moment

of the Senthil–Fisher single-vortex proposal for cuprates, and bridges the puzzling experiments in 4Hb-TaS$_2$ with the forefront of topological orders and their detection.

2 Magnetic memory effect of superconducting 4Hb-TaS$_2$

Due to various tunability and controllability of their physical properties, the TaS$_2$-based van der Waals materials [18] have attracted a great interest. Among these TaS$_2$-based systems, the superconducting 4Hb-TaS$_2$ recently received some experimental attention [16, 17, 19]. Differing from other TaS$_2$-based materials, the 4Hb-TaS$_2$ consists of an alternating stacking of 1T-TaS$_2$ and 1H-TaS$_2$ layers. Moreover, the octahedral 1T-TaS$_2$ and the trigonal prismatic 1H-TaS$_2$ layers have rather different physical properties. The multi-layered 1T-TaS$_2$ experiences a charge-density-wave (CDW) transition around 350 K. At even lower temperatures below 200 K, the system develops a commensurate CDW structure with a $\sqrt{13} \times \sqrt{13}$ structure. The 1T-TaS$_2$ layer can then be viewed as a triangular lattice of clusters of stars of David (see Fig. 1). In each cluster of star of David, there are 13 electrons and hence one unpaired electron. Due to the correlation, this unpaired electron forms an effective spin-1/2 local moment [20–22], and the system becomes a correlation-driven cluster Mott insulator [23–25]. The emergence of the local spin-1/2 moment was supported by the Kondo resonance in the Pb-doped 1T-TaS$_2$ [26]. It was further shown that, this cluster Mott insulator is a spinon Fermi surface U(1) spin liquid in the weak Mott regime [22], and is quite analogous to the triangular lattice spin liquid in the organic compounds κ-(ET)$_2$Cu$_2$(CN)$_3$ and EtMe$_3$Sb[Pd(dmit)$_2$]$_2$ [27, 28]. The muon-spin-relaxation (μSR) experiments indicated a gapless spin liquid dynamics and no long-range order down to 70 mK in the 1T-TaS$_2$ [29]. The scanning tunneling microscopy on the isostructural monolayer 1T-TaSe$_2$ identified interesting evidences of the spinon Fermi surface in the cluster Mott insulating regime [30, 31]. In contrast to the correlated insulating behavior in the 1T-TaS$_2$,

the 1H-TaS$_2$ layer develops the 3×3 CDW and is a good metal at low temperatures [17]. The bulk form of 1H-TaS$_2$, 2H-TaS$_2$, superconducts at 0.7 K. Once 1T-TaS$_2$ and 1H-TaS$_2$ layers are stacked together to form the bulk 4Hb-TaS$_2$ structure, the superconducting transition temperature T_c is greatly enhanced, reaching 2.7 K. This anomalous enhancement might arise from the charge transfer between the 1T and the 1H layers [16, 17, 19]. On the other hand, the insulating 1T-TaS$_2$ itself under the substitution of S with Se can superconduct with a maximal T_c about 3.5 K [32, 33]. Thus, it seems a bit unclear where the superconductivity originates from. The more surprising and important result, however, is the magnetic memory effect and the spontaneous vortex generation, and this is what we focus on below.

We sketch the magnetic memory effect and the spontaneous vortex generation in 4Hb-TaS$_2$. It was found that, the system generates a vortex lattice under the field cooling from above T_c to below T_c. After increasing the temperature above T_c and turning off the magnetic field, one finds that a subsequent zero-field coupling to the temperatures below T_c results in the superconducting vortices whose density is about one order of magnitude dilute than the field-cooling case. These vortices appeared spontaneously, suggesting an intrinsic magnetic memory of the system. This effect disappears when the thermal cycle reaches 3.6 K that is 0.9 K above T_c. The magnetic signal was found to be absent both below T_c (without the vortices) and above T_c [16], which may be a bit incompatible with the chiral spin liquid (CSL) scenario as the scalar spin chirality would induce a weak magnetization.

To understand the magnetic memory effect and the spontaneous vortex generation in 4Hb-TaS$_2$, we propose this physics is related to the $\mathbb{Z}_2$ topological order, and we expect the $\mathbb{Z}_2$ topological order to be relevant to the superconducting 4Hb-TaS$_2$. Here it does not really mean the $\mathbb{Z}_2$ topological order is the driving force for superconductivity, but simply suggests the potential relevance in this context. We start from the 1T-TaS$_2$ where the spinon Fermi surface U(1) spin liquid is suggested to be relevant [21, 22, 30]. The observation is that, once the electron pairing is introduced into the 1T-TaS$_2$ system, the system becomes a $\mathbb{Z}_2$ spin liquid with a $\mathbb{Z}_2$ topological order. This is simply understood from a single-band Hubbard model on a triangular lattice for the star of David clusters below,

$$H = \sum_{\langle ij \rangle} \left(-tc_{i\sigma}^{\dagger}c_{j\sigma} + \Delta c_{i\uparrow}^{\dagger}c_{j\downarrow}^{\dagger} + h.c. \right) + \sum_i Un_{i\uparrow}n_{i\downarrow}, \qquad (1)$$

where a uniform electron pairing is explicitly introduced. Here $c_{i\sigma}^{\dagger}$ ($c_{i\sigma}$) is the creation (annihilation) operator for the electron in the star-of-David cluster at the lattice site i, and $n_{i\alpha} \equiv c_{i\sigma}^{\dagger}c_{i\sigma}$. Although the effective model for 1T-TaS$_2$ in the cluster Mott insulating regime was suggested to be a

XXZ spin model with a XXZ-ring exchange term [22, 34], the single-band Hubbard model is sufficient to capture the strong charge fluctuations for the emergence of the spin liquid and may be more convenient for the discussion of the pairing. The 1T-TaS$_2$ is located near the Mott transition [22] and in the weak Mott insulating regime. Crudely speaking, this regime behaves like a metal at short distances, and is insulating at long distances.

This electron pairing may have several origins. It can arise from the electron-phonon coupling from either 1T-TaS$_2$ itself or the 1H layers. It can arise from the superconducting proximity effect from the 1H layers. It can also arise from the correlation effect in 1T-TaS$_2$ whose microscopic mechanism is less clear. In Ref. [35], gapless d-wave pairing states both with and without time reversal symmetry have actually been proposed. To capture the spin-charge separation in the weak Mott regime, we use the slave-rotor representation [36, 37] to express the electron operator as $c_{i\sigma} \equiv e^{-i\theta_i} f_{i\sigma}$ where $e^{-i\theta_i}$ annihilates the boson charge at i and $f_{i\sigma}$ is the annihilation operator for the fermionic spinon, and the Hamiltonian without the pairing becomes

$$H_{\Delta=0} = \sum_{\langle ij \rangle} \left[-t f_{i\sigma}^\dagger f_{j\sigma} e^{i\theta_i - i\theta_j} + h.c. \right] + \sum_i U n_{i\uparrow} n_{i\downarrow}. \qquad (2)$$

The slave-rotor representation enlarges the physical Hilbert space, and a Hilbert space constraint $L_i = \sum_\sigma f_{i\sigma}^\dagger f_{i\sigma}$ should be imposed where L_i is a conjugate angular momentum operator for the rotor. With a standard slave-rotor mean-field decoupling [37], one finds the system enters the Mott side when $U > 2.73t$. In the weak Mott regime, the system in the absence of pairing is in a spinon Fermi surface U(1) spin liquid with the mean-field spinon Hamiltonian,

$$H_{U(1)} = \sum_{\langle ij \rangle} \left[-t_s f_{i\sigma}^\dagger f_{j\sigma} + h.c. \right]. \qquad (3)$$

This mean-field result was equivalently established by working on the relevant exchange spin model for 1T-TaS$_2$ in the weak Mott regime [22] and can be regarded as the parent state for the 1T-TaS$_2$ structure. The electron pairing term, in the Mott regime, becomes the spinon pairing in the mean-field description,

$$c_{i\uparrow}^\dagger c_{j\downarrow}^\dagger \rightarrow f_{i\uparrow}^\dagger f_{j\downarrow}^\dagger \langle e^{i\theta_i + i\theta_j} \rangle, \qquad (4)$$

and the U(1) gauge theory is immediately higgsed down to $\mathbb{Z}_2$. The resulting $\mathbb{Z}_2$ spin liquid is simply described by

$$H_{\mathbb{Z}_2} = \sum_{\langle ij \rangle} \left[-t_s f_{i\alpha}^\dagger f_{j\alpha} + \Delta_s f_{i\uparrow}^\dagger f_{j\downarrow}^\dagger + h.c. \right], \qquad (5)$$
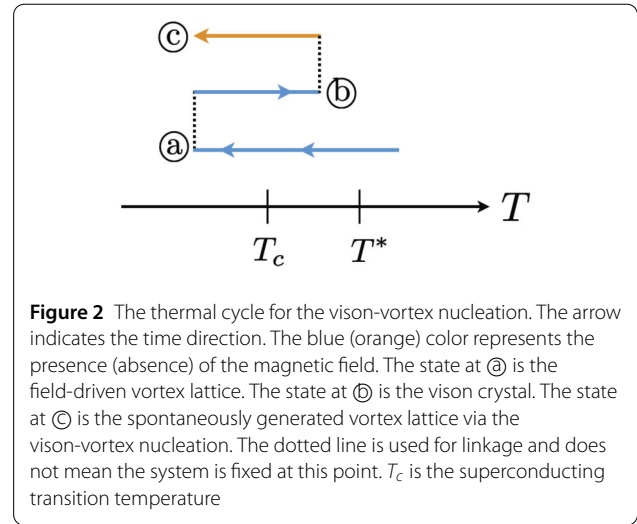

Figure 2 The thermal cycle for the vison-vortex nucleation. The arrow indicates the time direction. The blue (orange) color represents the presence (absence) of the magnetic field. The state at ⓐ is the field-driven vortex lattice. The state at ⓑ is the vison crystal. The state at ⓒ is the spontaneously generated vortex lattice via the vison-vortex nucleation. The dotted line is used for linkage and does not mean the system is fixed at this point. T_c is the superconducting transition temperature

where t_s (Δ_s) is the spinon hopping (pairing). We thus propose that the correlated 1T-TaS$_2$ layers in the superconducting environment are pertinent to the $\mathbb{Z}_2$ topological order. This is so as long as there exist electron pairings in the 1T-TaS$_2$ layers, and we think this is the root to understand the exotic physics in the 4Hb-TaS$_2$. Depending on the strength of the interlayer coupling, this system can either be a multi-layered two-dimensional $\mathbb{Z}_2$ topological order or be a three-dimensional $\mathbb{Z}_2$ topological order.

The magnetic memory effect and the spontaneous vortex generation in the 4Hb-TaS$_2$ can be understood from the proximity to the $\mathbb{Z}_2$ topological order. It is more convenient to discuss along the line of a three-dimensional $\mathbb{Z}_2$ topological order, and the two-dimensional $\mathbb{Z}_2$ topological order requires a bit more explanation as it cannot exist at any finite temperature. We follow the thermal cycle in Fig. 2 (that is also the experimental cycle in Ref. [16]) to describe the understanding from the $\mathbb{Z}_2$ topological order. The field cooling to the temperature below T_c generates a large number of vortices in the form of vortex lattice (that corresponds to the state ⓐ in Fig. 2). After raising the temperature above T_c, the magnetic field enters the system and the superconducting vortices just disappear. But the visons that are connected to the superconducting vortices could remain in the system with the three-dimensional $\mathbb{Z}_2$ topological order as long as the temperature is below the vison-unbinding transition at T^*. The superconducting vortex only has one sign once the field direction is fixed. But the vison has a $\mathbb{Z}_2$ structure, and thus, a pair of visons can annihilate each other. In the three-dimensional $\mathbb{Z}_2$ topological order, the visons appear as the vison loops or vison lines. This corresponds to the state ⓑ. Before the vison lines come together and annihilate each other in the vison crystal, one cools the system back to the superconducting regime in the absence of the magnetic field. The vison crystal will nucleate back into the superconducting

vortices (i.e. state ⓒ in Fig. 2). This is a layered material, the nucleated vortices have a natural orientation. The sign of the flux for the vortices is selected by the residual magnetic field from the environment. This spontaneous vortex generation will disappear if the temperature is raised above T^* or the time internal for the system above T_c is too long such that the visons have already annihilated completely. If one performs the experiment with a single or odd number of vortices, the consequence of this annihilation will always end up with one residual vison, and thus, one would always obtain a single nucleated vortice. In the discussion part, we mention the modification with the multi-layered two-dimensional $\mathbb{Z}_2$ topological order where the vison-vortex nucleation idea stays invariant.

3 Distinction from chiral spin liquid scenario

We suggest further experiments to distinguish the proposal with the $\mathbb{Z}_2$ topological order from the proposal with the chiral spin liquid (CSL). The CSL was proposed numerically for the triangular lattice Hubbard model in the weak Mott regime and was theoretically analyzed [38, 39]. The time reversal symmetry breaking with the scalar spin chirality was shown to arise from the ring exchange interaction that can be thought as the products of the scalar spin chiralities [39]. Due to the connection between the 1T-TaS$_2$ and the triangular lattice Hubbard model and/or the ring exchange model, such a CSL may have a relevance with the superconducting 4Hb-TaS$_2$. As the CSL breaks time reversal symmetry and time reversal symmetry is an Ising symmetry, there should be a finite temperature transition. In addition, there exists a uniform distribution of the scalar spin chirality throughout the triangular lattice that corresponds to the emergent U(1) gauge flux distribution with a $\pi/2$ flux on each triangle and π flux on each unit cell. In the CSL, the spinon is already fully gapped. Moreover, due to the presence of the background π flux, the translation symmetry is realized projectively for the spinons, and the spinon continuum that is detectable by the inelastic neutron scattering experiments would have an enhanced spectral periodicity in the Brillouin zone [4, 40–42]. To reveal this, we combine a generic argument [42] with the calculation by fixing the gauge according to Fig. 3.

3.1 Spectral periodicity of spinon continuum in chiral spin liquid

One first defines the two lattice translation operations T_1 and T_2, where the T_1 (T_2) operation translates the system by the triangular lattice vector $\boldsymbol{a}_1$ ($\boldsymbol{a}_2$). According to Fig. 3 in the main text. we have

$$\boldsymbol{a}_1 = (1,0), \tag{6}$$

$$\boldsymbol{a}_2 = \left(-\frac{1}{2}, \frac{\sqrt{3}}{2}\right). \tag{7}$$

For the chiral spin liquid, the spinons are defined and fractionalized excitations, in addition to the fractional statistics. The symmetry is again fractionalized, and more precisely, the symmetry operation acts locally the spinons. For the translation symmetry, if we translate the spinon around the parallelogram formed by $\boldsymbol{a}_1$ and $\boldsymbol{a}_2$, the spinon will experience the background π flux [2, 40, 42], i.e.

$$\left(T_2^s\right)^{-1}\left(T_1^s\right)^{-1}T_2^s T_1^s = -1, \tag{8}$$

where the superscript 's' merely refers to the spinon symmetry operation. Thus, for the spinon, these two translation operations anticommute with each other with,

$$T_1^s T_2^s = -T_2^s T_1^s. \tag{9}$$

The translation symmetry fractionalization and the anticommutation relation between the two translation operations immediately lead to an enhanced spectral periodicity of the spinon continuum in the chiral spin liquid. To show that, we extend the $\mathbb{Z}_2$ topological order of the square lattice example in Ref. [42] to the triangular lattice and consider a generic two-spinon scattering state,

$$|a\rangle \equiv |\boldsymbol{q}_a, m_a\rangle, \tag{10}$$

where $\boldsymbol{q}_a$ refers to the crystal momentum of this state $|a\rangle$, and m_a labels the rest quantum number to characterize this state. Because the Bravais lattice vectors of the triangular lattice are not orthogonal, we expand the crystal momentum $\boldsymbol{q}_a$ in the nonorthogonal basis in the reciprocal space with

$$\boldsymbol{q}_a = q_{a1}\boldsymbol{e}_1 + q_{a2}\boldsymbol{e}_2, \tag{11}$$

where the basis vectors are given as

$$\boldsymbol{e}_1 = \left(0, \frac{2}{\sqrt{3}}\right), \tag{12}$$

$$\boldsymbol{e}_2 = \left(1, \frac{1}{\sqrt{3}}\right). \tag{13}$$

Based on the symmetry fractionalization and the symmetry localization, we apply the lattice translation on the two-spinon scattering state and obtain,

$$T_\mu |a\rangle = T_\mu^s(s1) T_\mu^s(s2) |a\rangle. \tag{14}$$

Here 's1' and 's2' refer to two spinons, and the translation operation T_μ is fractionalized to two spinon operations T_μ^s. We then apply the spinon translation operation on the spinon $s1$ of the two-spinon scattering state $|a\rangle$ to generate other two equal energy spinon scattering states, i.e.,
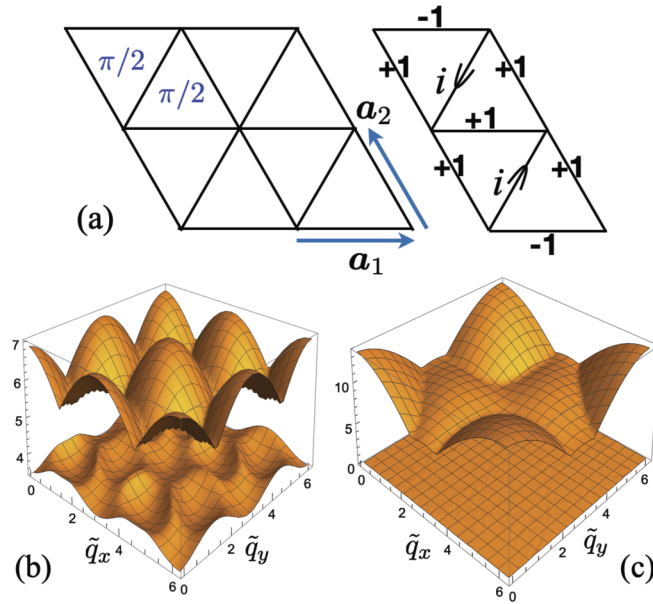
$$|b\rangle = T_1^s(s1)|a\rangle, \tag{15}$$

Figure 3 (a) The gauge flux pattern in the CSL and its gauge fixing (that is repeated along $\boldsymbol{a}_1$ direction). The length of the lattice vectors is set to unity. The upper and lower excitation edges of the spinon continuum for the CSL in (b) and for the $\mathbb{Z}_2$ topological order of Eq. (5) in (c). The energy unit is set to t_s, and $\Delta_s = 0.2t_s$. For our convenient, we have defined $\tilde{q}_x \equiv \boldsymbol{q} \cdot \boldsymbol{a}_1$ and $\tilde{q}_y \equiv \boldsymbol{q} \cdot \boldsymbol{a}_2$.

$$|c\rangle = T_2^s(s1)|a\rangle. \tag{16}$$

To show that these spinon scattering states have distinct crystal momenta, we apply the lattice translation operation on these states and compare the eigenvalues,

$$T_1|b\rangle = T_1^s(s1)T_1^s(s2)T_1^s(s1)|a\rangle = +T_1^s(s1)\big[T_1|a\rangle\big], \tag{17}$$

$$T_2|b\rangle = T_2^s(s1)T_2^s(s2)T_1^s(s1)|a\rangle = -T_1^s(s1)\big[T_2|a\rangle\big]. \tag{18}$$

In Eq. (18), the anticommutation relation in Eq. (9) has been used. The above relations indicates that,

$$q_{b1} = q_{a1}, \qquad q_{b2} = q_{a2} + \pi. \tag{19}$$

With a similar construction, we find that,

$$T_1|c\rangle = -T_2^s(s1)\big[T_1|a\rangle\big], \tag{20}$$

$$T_2|c\rangle = +T_2^s(s1)\big[T_2|a\rangle\big]. \tag{21}$$

Thus, we have

$$q_{c1} = q_{a1} + \pi, \qquad q_{c2} = q_{a2}. \tag{22}$$

These two-spinon scattering states have the same energy, and the relation between their crystal momenta indicates that there is an enhanced spectral periodicity in the spinon continuum. Both the lower and upper excitation edges of

the spinon continuum have this spectral periodicity enhancement with

$$\mathcal{L}[\boldsymbol{q}] = \mathcal{L}[\boldsymbol{q} + \pi\boldsymbol{e}_1] = \mathcal{L}[\boldsymbol{q} + \pi\boldsymbol{e}_2], \tag{23}$$

$$\mathcal{U}[\boldsymbol{q}] = \mathcal{U}[\boldsymbol{q} + \pi\boldsymbol{e}_1] = \mathcal{U}[\boldsymbol{q} + \pi\boldsymbol{e}_2]. \tag{24}$$

An explicit calculation of the spinon continuum for the chiral spin liquid is given in the following.

3.2 Distinction in spinon continuum

As we have discussed in details above, both the lower excitation edge, $\mathcal{L}[\boldsymbol{q}]$, and the upper excitation edge, $\mathcal{U}[\boldsymbol{q}]$, of the spinon continuum develop an enhanced spectral periodicity. These two edges are the energy bounds for the spinon continuum, and we have

$$\mathcal{L}[\boldsymbol{q}] = \mathcal{L}\left[\boldsymbol{q} + \pi\left(0, \frac{2}{\sqrt{3}}\right)\right] = \mathcal{L}\left[\boldsymbol{q} + \pi\left(1, \frac{1}{\sqrt{3}}\right)\right], \tag{25}$$

$$\mathcal{U}[\boldsymbol{q}] = \mathcal{U}\left[\boldsymbol{q} + \pi\left(0, \frac{2}{\sqrt{3}}\right)\right] = \mathcal{U}\left[\boldsymbol{q} + \pi\left(1, \frac{1}{\sqrt{3}}\right)\right]. \tag{26}$$

For the explicit calculation, we consider the following mean-field spinon Hamiltonian for the two-dimensional CSL,

$$H_{\mathrm{CSL}} = \sum_{\langle ij\rangle}\big[-t_s e^{i\phi_{ij}}f_{i\alpha}^{\dagger}f_{j\alpha} + h.c.\big], \tag{27}$$

where the phase $e^{i\phi_{ij}}$ is chosen according to Fig. 3. The spinons have two bands and the dispersions are given as

$$\omega_{\pm}(\boldsymbol{q}) = \pm t_s \Big[2\big(3 + \cos(2\boldsymbol{q} \cdot \boldsymbol{a}_1) + \cos(2\boldsymbol{q} \cdot \boldsymbol{a}_2) + \cos(2\boldsymbol{q} \cdot \boldsymbol{a}_1 + 2\boldsymbol{q} \cdot \boldsymbol{a}_2)\big) \Big]^{1/2}. \tag{28}$$

The lowest spinon band carries a Chern number $C = 1$, and is fully filled. The gapped spinon continuum $\Omega(\boldsymbol{q})$ is obtained from $\boldsymbol{q} = \boldsymbol{q}_1 - \boldsymbol{q}_2$ and $\Omega(\boldsymbol{q}) = \omega_+(\boldsymbol{q}_1) - \omega_-(\boldsymbol{q}_2)$, and is plotted in Fig. 3.

As a comparison, we compute the spinon continuum for the $\mathbb{Z}_2$ topological order on the triangular lattice from Eq. (5). As this state is derived from the spinon Fermi surface state with the uniform hopping by introducing the pairing, we do not expect the spectral periodicity enhancement (see Fig. 3). Nevertheless, due to the weak uniform pairing, the spectral weight of the weakly gapped spinon continuum may still carry the "$2k_F$" features of the spinon Fermi surface [22].

3.3 Other distinctions
In addition to the distinction between the spectral periodicity in the spinon continuum, the thermal Hall effect is another clear experimental probe to distinguish the $\mathbb{Z}_2$ topological order from the CSL. Due to the finite Chern number of the filled spinon band in the CSL, there exists a chiral (charge-neutral) edge state that does not really conduct charge but conduct heat. One expects a quantized thermal Hall effect with

$$\kappa_{xy}/T = \frac{\pi}{3} k_B^2/\hbar, \tag{29}$$

even in the absence of magnetic field, and the gauge fluctuations do not change the order of magnitude of κ_{xy}/T [43]. To avoid the complication from the superconducting vortices, one may carry the measurement above T_c. This quantized thermal Hall effect should be a large signal if the CSL is relevant for the 4Hb-TaS$_2$. Since there exists the charge transfer between the layers in 4Hb-TaS$_2$, one further expects a topological Hall effect from the charge carriers, where the charge carriers experience the scalar spin chirality from the CSL as the real-space Berry phase and produce the Hall effect. In contrast, both anomalous Hall effect and thermal Hall effect should be absent in our proposal for the $\mathbb{Z}_2$ topological order, except if the superconducting phase has a weak time reversal symmetry breaking [35, 44], and the signals may be quite weak compared to the quantized one in the CSL scenario.

4 Discussion
We compare the vison-vortex nucleation idea with the vortex lattice here and the single vortex case in the Senthil–Fisher cuprate proposal [9]. In the cuprate proposal,

Senthil and Fisher considered a single $hc/2e$ vortex. The system leaves the superconducting regime, the single vison puts the system in a distinct superselection sector of the $\mathbb{Z}_2$ topological order, and the single vison cannot annihilate itself. Once the system reenters the superconducting regime, the vison would nucleate into a superconducting vortices. They further argued that, as long as the number of vortices is odd, there will be one vison remaining and the phenomenon will be there. For the case of the vortex lattice that we discuss in this Letter, once the system leaves the superconducting regime but remains in the $\mathbb{Z}_2$ topologically ordered regime, the visons in the vison crystal would annihilate with each other. But if this time for the vison crystal to be fully annihilated is longer than the time interval for the experiments to return to the superconducting regime, the remaining visons will nucleate back to the superconducting vortices. This seems to be what has happened in the superconducting 4Hb-TaS$_2$ [16]. Thus the vortex lattice with many vortices makes the experimental phenomena much more visible than a single vortex.

The three-dimensional $\mathbb{Z}_2$ topological order has a finite temperature phase transition from the vison loop unbinding. This transition is an Ising transition, and sets the upper temperature for the magnetic memory effect. Indeed, in the low-temperature thermodynamic measurement in the 4Hb-TaS$_2$, only the superconducting transition is clearly visible [44], and the upper temperature for the magnetic memory effect is 3.6 K, a bit above T_c. Due to the layered structure, it is also possible, the $\mathbb{Z}_2$ topological order is two dimensional. In such a case, strictly speaking, the topological order cannot exist at any finite temperature. Similar to what has been argued by Senthil and Fisher for the single vison, the vison crystal, however, can be present for a finite time before escaping. In this case, besides the vison annihilation effect, the vison gap sets a crossover temperature scale for the upper temperature for the magnetic memory effect.

For the chiral spin liquid scenario, one may invoke the anyon superconductivity. As the anyon naturally carries the intrinsic flux, one may establish the connection between the anyon excitations and the superconducting vortices in a way analogous to the vison and the vortex. In the state ⓑ in Fig. 2, one would expect an anyon crystal of some sort. We will come back to this theoretical possibility in the future work.

Since we expect the $\mathbb{Z}_2$ topological order arises from the correlation physics of the 1T-TaS$_2$ layers, it is natural for us to vision that a similar magnetic memory effect and the spontaneous vortex generation could occur in the Se-doped 1T-TaS$_2$ where the superconductivity is also obtained [32, 33].

To summarize, we associate the puzzling magnetic memory effect and the spontaneous vortex generation in the 4Hb-TaS$_2$ to the vison-vortex nucleation from the $\mathbb{Z}_2$ topological order, and suggest other experimental phenomena

to distinguish this proposal from the chiral spin liquid scenario.

Declarations

Competing interests
Gang V. Chen is an editorial board member for Quantum Frontiers and was not involved in the editorial review, or the decision to publish, this article. Both authors declare that there are no competing interests.

Author details
[1]International Center for Quantum Materials, School of Physics, Peking University, Beijing, 100871, China. [2]Department of Physics and HKU-UCAS Joint Institute for Theoretical and Computational Physics at Hong Kong, The University of Hong Kong, Hong Kong, China. [3]Collaborative Innovation Center of Quantum Matter, Beijing, 100871, China.

References

1. Wen X-G (2013) Topological order: from long-range entangled quantum matter to a unified origin of light and electrons. ISRN Condens Matter Phys 2013:1–20
2. Wen X-G (2002) Quantum orders and symmetric spin liquids. Phys Rev B 65:165113
3. Mesaros A, Ran Y (2013) Classification of symmetry enriched topological phases with exactly solvable models. Phys Rev B 87:155115
4. Essin AM, Hermele M (2013) Classifying fractionalization: symmetry classification of gapped $\mathbb{Z}_2$ spin liquids in two dimensions. Phys Rev B 87:104406
5. Kitaev A (2006) Anyons in an exactly solved model and beyond. Ann Phys 321:2–111
6. Laughlin RB (1983) Anomalous quantum Hall effect: an incompressible quantum fluid with fractionally charged excitations. Phys Rev Lett 50:1395–1398
7. Arovas D, Schrieffer JR, Wilczek F (1984) Fractional statistics and the quantum Hall effect. Phys Rev Lett 53:722–723
8. Senthil T, Fisher MPA (2000) Z_2 gauge theory of electron fractionalization in strongly correlated systems. Phys Rev B 62:7850–7881
9. Senthil T, Fisher MPA (2001) Fractionalization in the cuprates: detecting the topological order. Phys Rev Lett 86:292–295
10. Balents L, Fisher MPA, Nayak C (2000) Dual vortex theory of strongly interacting electrons: a non-Fermi liquid with a twist. Phys Rev B 61:6307–6319
11. Balents L, Fisher MPA, Nayak C (1999) Dual order parameter for the nodal liquid. Phys Rev B 60:1654–1667
12. Motrunich OI, Senthil T (2005) Origin of artificial electrodynamics in three-dimensional bosonic models. Phys Rev B 71:125102
13. Senthil T (2015) Symmetry-protected topological phases of quantum matter. Annu Rev Condens Matter Phys 6:299–324
14. Chen G (2016) "Magnetic monopole" condensation of the pyrochlore ice U(1) quantum spin liquid: application to $Pr_2Ir_2O_7$ and $Yb_2Ti_2O_7$. Phys Rev B 94:205107
15. Bonn DA, Wynn JC, Gardner BW, Lin Y-J, Liang R, Hardy WN, Kirtley JR, Moler KA (2001) A limit on spin–charge separation in high-T_c superconductors from the absence of a vortex-memory effect. Nature 414:887–889
16. Persky E, Bjørlig AV, Feldman I, Almoalem A, Altman E, Berg E, Kimchi I, Ruhman J, Kanigel A, Kalisky B (2022) Magnetic memory and spontaneous vortices in a van der Waals superconductor. Nature 607:692–696
17. Shen S, Wen C, Kong P, Gao J, Si J, Luo X, Lu W, Sun Y, Chen G, Yan S (2022) Inducing and tuning kondo screening in a narrow-electronic-band system. Nat Commun 13. https://doi.org/10.1038/s41467-022-29891-4
18. Hossain M, Zhao Z, Wen W, Wang X, Wu J, Xie L (2017) Recent Advances in Two-Dimensional Materials with Charge Density Waves: synthesis, Characterization and Applications. Crystals 7. https://doi.org/10.3390/cryst7100298
19. Kumar Nayak A, Steinbok A, Roet Y, Koo J, Margalit G, Feldman I, Almoalem A, Kanigel A, Fiete GA, Yan B, Oreg Y, Almoalem N, Beidenkopf H, (2021) Evidence of topological boundary modes with topological nodal-point superconductivity. Nat Phys 17:1413–1419
20. Law KT, Lee PA (2017) 1T-TaS$_2$ as a quantum spin liquid. Proc Natl Acad Sci 114:6996–7000
21. Li C-K, Yao X-P, Liu J, Chen G (2022) Fractionalization on the surface: is type-II terminated 1T-TaS$_2$ surface an anomalously realized spin liquid? Phys Rev Lett 129:017202
22. He W-Y, Yan Xu X, Chen G, Law KT, Lee PA (2018) Spinon Fermi surface in a cluster Mott insulator model on a triangular lattice and possible application to 1T-TaS$_2$. Phys Rev Lett 121:046401
23. Chen G, Lee PA (2018) Emergent orbitals in the cluster Mott insulator on a breathing Kagome lattice. Phys Rev B 97:035124
24. Chen G, Kee H-Y, Baek Kim Y (2016) Cluster Mott insulators and two Curie-Weiss regimes on an anisotropic Kagome lattice. Phys Rev B 93:245134
25. Yao X-P, Zhang X-T, Baek Kim Y, Wang X, Chen G (2020) Clusterization transition between cluster Mott insulators on a breathing Kagome lattice. Phys Rev Res 2:043424
26. Shen S, Qin T, Gao J, Wen C, Wang J, Wang W, Li J, Luo X, Lu W, Sun Y, Yan S (2022) Coexistence of quasi-two-dimensional superconductivity and tunable Kondo lattice in a van der Waals superconductor. Chin Phys Lett 39:077401
27. Kurosaki Y, Shimizu Y, Miyagawa K, Kanoda K, Saito G (2005) Mott transition from a spin liquid to a Fermi liquid in the spin-frustrated organic conductor κ-(ET)$_2$Cu$_2$(CN)$_3$. Phys Rev Lett 95:177001
28. Itou T, Oyamada A, Maegawa S, Tamura M, Kato R (2008) Quantum spin liquid in the spin-1/2 triangular antiferromagnet EtMe$_3$Sb[Pd(dmit)$_2$]$_2$. Phys Rev B 77:104413
29. Klanjšek M, Zorko A, Žitko R, Mravlje J, Jagličić Z, Kumar Biswas P, Prelovšek P, Mihailovic D, Arčon D (2017) A high-temperature quantum spin liquid with polaron spins. Nat Phys 13:1130–1134
30. Wei R, Chen Y, Tang S, Hwang J, Tsai H-Z, Lee RL, Wu M, Ryu H, Kahn S, Liou F, Jia C, Aikawa A, Hwang C, Wang F, Choi Y, Louie SG, Lee PA, Shen Z-X, Mo S-K, Crommie MF (2021) Evidence for quantum spin liquid behaviour in single-layer 1T-TaSe$_2$ from scanning tunnelling microscopy. Nat Phys 17:1154–1161
31. Chen Y, He W-Y, Ruan W, Hwang J, Tang S, Lee RL, Wu M, Zhu T, Zhang C, Ryu H, Wang F, Louie SG, Shen Z-X, Mo S-K, Lee PA, Crommie MF (2022) Evidence for a spinon Kondo effect in cobalt atoms on single-layer 1T-TaSe$_2$. Nat Phys 18:1335–1340
32. Qiao S, Li X, Wang N, Ruan W, Ye C, Cai P, Hao Z, Yao H, Chen X, Wu J, Wang Y, Liu Z (2017) Mottness collapse in 1T-TaS$_{2-x}$Se$_x$ transition-metal dichalcogenide: an interplay between localized and itinerant orbitals. Phys Rev X 7:041054
33. Ang R, Wang ZC, Chen CL, Tang J, Liu N, Liu Y, Lu WJ, Sun YP, Mori T, Ikuhara Y (2015) Atomistic origin of an ordered superstructure induced superconductivity in layered chalcogenides. Nat Commun 6:6091
34. Motrunich OI (2005) Variational study of triangular lattice spin-1/2 model with ring exchanges and spin liquid state in κ-(ET)$_2$Cu$_2$(CN)$_3$. Phys Rev B 72:045105

35. Mishmash RV, Garrison JR, Bieri S, Xu C (2013) Theory of a competitive spin liquid state for weak Mott insulators on the triangular lattice. Phys Rev Lett 111:157203

36. Florens S, Georges A (2004) Slave-rotor mean-field theories of strongly correlated systems and the Mott transition in finite dimensions. Phys Rev B 70:035114

37. Lee S-S, Lee PA (2005) U(1) gauge theory of the Hubbard model: spin liquid states and possible application to κ-(ET)$_2$Cu$_2$(CN)$_3$. Phys Rev Lett 95:036403

38. Szasz A, Motruk J, Zaletel MP, Moore JE (2020) Chiral spin liquid phase of the triangular lattice Hubbard model: a density matrix renormalization group study. Phys Rev X 10:021042

39. Cookmeyer T, Motruk J, Moore JE (2021) Four-spin terms and the origin of the chiral spin liquid in Mott insulators on the triangular lattice. Phys Rev Lett 127:087201

40. Chen G (2017) Spectral periodicity of the spinon continuum in quantum spin ice. Phys Rev B 96:085136

41. Chen G (2017) Dirac's "magnetic monopoles" in pyrochlore ice U(1) spin liquids: spectrum and classification. Phys Rev B 96:195127

42. Essin AM, Hermele M (2014) Spectroscopic signatures of crystal momentum fractionalization. Phys Rev B 90:121102

43. Guo H, Samajdar R, Scheurer MS, Sachdev S (2020) Gauge theories for the thermal Hall effect. Phys Rev B 101:195126

44. Ribak A, Majlin Skiff R, Mograbi M, Rout PK, Fischer MH, Ruhman J, Chashka K, Dagan Y, Kanigel A (2020) Chiral superconductivity in the alternate stacking compound 4Hb-TaS$_2$. Sci Adv 6:eaax9480. https://www.science.org/doi/pdf/10.1126/sciadv.aax9480

Publisher's Note

Springer Nature remains neutral with regard to jurisdictional claims in published maps and institutional affiliations.